Propagation of Microwaves in a Circular Waveguide Partially Filled with a Cold Plasma Dielectric

O. Gehre, H. M. Mayer, and M. Tutter

Max-Planck-Institut für Plasmaphysik, Garching, Germany

The dispersion of microwaves propagating through a circular waveguide partially filled with a homogeneous lossless and cold electron plasma has been studied. Quantitative dispersion curves have been computed for the lowest radial modes of circular and dipole symmetry without using the quasistatic approximation. The curves comprise both "fast" or "waveguide" modes and "slow" or "plasmaguide" modes. Easily applicable approximations for the lowest waveguide modes are given.

Introduction

The propagation of microwaves in waveguides containing plasmas has already been studied extensively in the literature of the last decade. For a bibliography we quote Ref. [1,2].

The early work of Trivelpiece and Gould [3] was primarily dealing with a magnetized plasma. The results for the nonmagnetized plasma were limited to frequencies $\omega < \omega_p/\sqrt{2}$ and in most cases to the quasistatic approximation ($2b \ll \lambda_0$, $\lambda_0 = $ vacuum wavelength). In this manner thermal effects have also been treated [4]. When dealing with an experiment on the Fresnel dragging effect of a glow discharge on 3 cm microwaves [5,6] the authors found that the case $\omega > \omega_p$ did not receive much attention in the literature in spite of its diagnostic importance. The intention of the present paper is to fill this gap and to widen the already existing picture of plasma loaded waveguides by a coherent treatment of the two cases $\omega \gtrless \omega_p$.

Restricting ourselves to non-magnetized plasmas in cylindrical waveguides the simplest way to account for plasma inhomogeneity is to assume a profile of the dielectric constant given by [7]

$$\varepsilon(r) = \begin{cases} \varepsilon_1 = 1 - \omega_p^2/\omega^2 & \text{for} \quad 0 \leqq r \leqq a \\ \varepsilon_2 = 1 & \text{for} \quad a < r \leqq b \end{cases} \qquad (1)$$

where a and b are the radii of the plasma core and the waveguide respectively. We have neglected collisions and thermal motion of the electrons. Under these assumptions the $\omega(k)$ dependence is obtained from the solution of a boundary value problem discribed in textbooks [8,9].

The Electromagnetic Dispersion Relation

Following the methods outlined in [1,8,9] one can solve Maxwell's equations for the dielectric profile given by Eq. (1). The following set of equations determines the components of the wavenumber vector in the two dielectric regions.

$$k_z^2 = \varepsilon_1 k_0^2 - k_1^2, \qquad (2)$$

$$k_z^2 = \varepsilon_2 k_0^2 - k_2^2, \qquad (3)$$

$$\frac{\varepsilon_1}{\varepsilon_2} = \frac{m^2(k_2^2 - k_1^2) - \lambda(k_2^2 \varkappa - k_1^2 \mu)}{m^2(k_2^2 - k_1^2) - \varkappa(k_2^2 \varkappa - k_1^2 \mu)} \frac{k_1^2}{k_2^2} \qquad (4)$$
$$= \eta(k_1^2, k_2^2; a, b)$$

where the symbols have the following meaning:

$k_0 \;\; = \omega/c = $ vacuum wavenumber,

$k_{1,2} = $ radial wavenumbers in the inner and outer region respectively,

$k_z \;\; = $ axial wavenumber,

$m \;\;\; = $ azimuthal mode number determining the angular dependence $\propto \exp(i\,m\,\varphi)$,

$$\varkappa = a\,k_1 \frac{J'_m(a\,k_1)}{J_m(a\,k_1)}, \qquad (5)$$

$$\lambda = a\,k_2 \frac{J'_m(a\,k_2)\,N_m(b\,k_2) - N'_m(ak_2)\,J_m(b\,k_2)}{J_m(a\,k_2)\,N_m(b\,k_2) - N_m(a\,k_2)\,J_m(b\,k_2)}, \qquad (6)$$

$$\mu = a\,k_2 \frac{J'_m(a\,k_2)\,N'_m(b\,k_2) - N'_m(a\,k_2)\,J'_m(b\,k_2)}{J_m(a\,k_2)\,N'_m(b\,k_2) - N_m(a\,k_2)\,J'_m(b\,k_2)}. \qquad (7)$$

In the last equations primes denote derivatives with respect to the argument of the corresponding Bessel (or Neumann) function. Eqs. (2) and (3) simply express the splitting of a wave vector of absolute magnitude $\varepsilon^{1/2} k_0$ into a radial and an axial component, the latter being the same in the two dielectric regions. Eq. (4) is thedeterminantal equa-

tion[1] which assures the continuity of the tangential field components at the dielectric interface. Considering k_0, ε_1, ε_2 and the two radii a and b to be known, solution of Eqs. (2), (3) and (4) yields the unknown quantities k_1, k_2 and k_z.

The physical fact, that for vanishing losses the radial dependence must be described by standing waves in which both signs of $k_{1,2}$ play an equivalent role requires that these equations depend only on the squares of k_1 and k_2. Correspondingly only even functions like $\varkappa$, λ, μ and the squares of wavenumbers have been introduced into Eqs. (2) to (3). As the functions $\varkappa$, λ, μ are cylindrical analogues of $x \cdot \mathrm{tg}(x)$ and $x \cdot \mathrm{ctg}(x)$ with an alternating succession of zeros and poles the solution will be multivalued and results in an infinite number of possible radial modes.

Subtracting of Eqs. (2) and (3) from each other yields

$$k_2^2 - k_1^2 = k_0^2(\varepsilon_2 - \varepsilon_1) = k_p^2. \qquad (8)$$

For the profile given by Eq. (1) k_p has the frequency independent value ω_p/c and may be used as a reciprocal unit length. Introducing

$$s = b\,k_1; \qquad t = b\,k_2 \qquad (9)$$

we can rewrite Eqs. (8) and (4)

$$s^2 = t^2 - b^2\,k_p^2, \qquad (10)$$

$$\frac{\omega_p^2}{\omega^2} = 1 - \eta = 1 - \frac{m^2\,b^2\,k_p^2 - \lambda(t^2\varkappa - s^2\,\mu)}{m^2\,b^2\,k_p^2 - \varkappa(t^2\varkappa - s^2\,\mu)}\,\frac{s^2}{t^2}, \quad (11)$$

and thereby calculate directly the dependence of the normalized frequency ω/ω_p on the normalized wavenumber t for given values of the normalized density $(b\,k_\mathrm{p})^2$ and the geometric ratio a/b. The latter appears in $\varkappa$, λ and μ according to their definitions by Eqs. (5) to (7) when the quantities s and t from Eq. (9) are introduced in the arguments. Radial dispersion curves obtained from Eqs. (10) and (11) are shown in Figs. 1a and 1b.

Since ω/ω_p is now known for given t it is easy to obtain the axial wavenumber from Eq. (3)

$$(b\,k_z)^2 = (b\,k_0)^2 - t^2 = b^2\,k_p^2\,(\omega^2/\omega_p^2) - t^2. \quad (12)$$

The three last equations are an explicit representation of the dispersion relation in terms of the parameter t^2. Variation of t^2 from $-\infty$ to ∞ produces all radial modes. The possibility to calculate the dispersion by this simple procedure is a particularity of the density profile (1) with $\varepsilon_2 = 1$
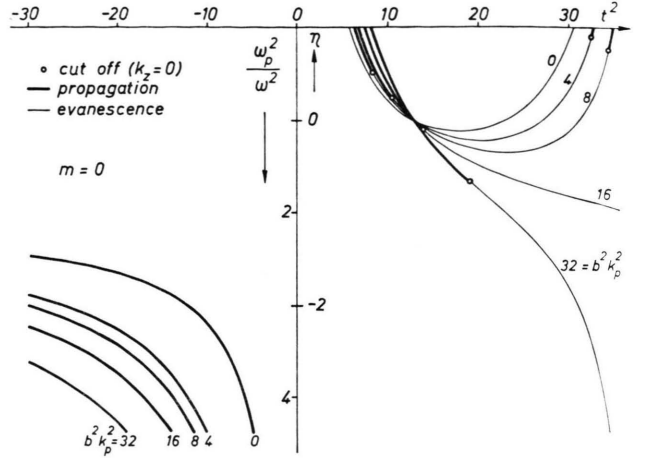

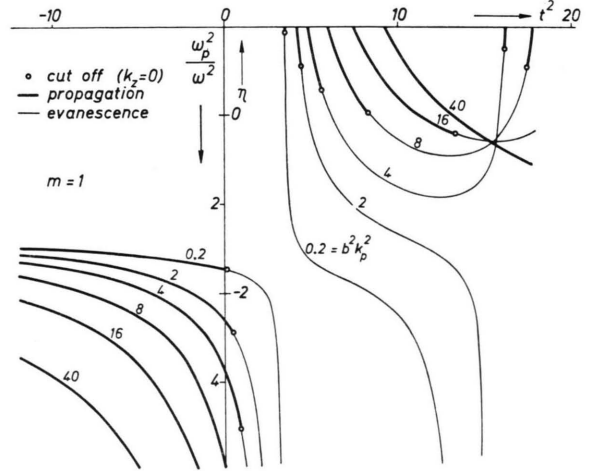Fig. 1a. Radial dispersion curves for $m = 0$, $a/b = 1/2$ and different values of the density parameter $b^2\,k_\mathrm{p}^2$.

Fig. 1b. Radial dispersion curves for $m = 1$, $a/b = 1/2$ and different values of $b^2\,k_\mathrm{p}^2$.

which according to Eq. (8) makes k_p frequency independent.

For $\varepsilon_2 \neq 1$ k_p^2 as defined by Eq. (8) will be given by

$$k_p^2 = k_0^2(\varepsilon_2 - \varepsilon_1) = \varepsilon_2\,k_0^2(1 - \eta) = \frac{\omega_p^2}{c^2}\,\frac{1 - \eta}{1 - \varepsilon_2\,\eta}\,\varepsilon_2\,. $$
$$(8\,\mathrm{a})$$

In order to apply curves of the kind shown in Figs. 1a and 1b to this case we calibrate the ordinate in units of the ratio $\varepsilon_1/\varepsilon_2 = \eta$ given by Eq. (4). We can now choose a pair of parameters (k_p^2, η) which satisfy Eq. (8a) and then find t^2 and k_z^2 in the manner already described. Once we have calculated a sufficiently dense array of curves η vs. t^2 at fixed a/b and various $(b\,k_p)^2$ for $\varepsilon = 1$,

we can construct step by step the dispersion relation $(\omega/\omega_p)^2$ vs. t^2 for the general case $\varepsilon_2 \neq 1$.

We have shown so far the general way in which the axial dispersion is obtained via the radial dispersion on the basis of Eqs. (9) to (12). Particular interest will deserve the conditions under which k_z vanishes (cut-off) or becomes infinite (resonance):

Cut-off $(k_z = 0)$

For $k_z = 0$ Eqs. (2) to (4) reduce to

$$k_1^2 = \varepsilon_1 k_0^2 \,. \tag{13}$$

$$k_2^2 = \varepsilon_2 k_0^2 \tag{14}$$

and

$$(\varkappa - \lambda)[(\varkappa/s^2) - (\mu/t^2)] = 0 \,. \tag{15}$$

At cut-off the left side of the determinantal equation splits into two factors. When setting up the full determinantal equation (Ref. [1], p. 216) we can trace back their origin and find that we can distinguish between "electric" cut-off at which the mode is of electric (TM) type and "magnetic" cut-off at which the mode is of magnetic (TE) type.

We have electric cut-off for

$$\varkappa = \lambda \tag{16}$$

and magnetic cut-off for

$$\varkappa/s^2 = \mu/t^2 \,. \tag{17}$$

Resonance $(k_z \to \infty)$

For large arguments we can use the asymptotic representations

$$J_m(z) = \left(\frac{2}{\pi z}\right)^{1/2} \cos\left(z - \frac{m\pi}{2} - \frac{\pi}{4}\right)$$
$$|z| \to \infty, \quad |\arg z| < \pi \tag{18}$$

$$N_m(z) = \left(\frac{2}{\pi z}\right)^{1/2} \sin\left(z - \frac{m\pi}{2} - \frac{\pi}{4}\right)$$

in Eqs. (5) to (7). In particular for large imaginary values of k_1 and k_2 we obtain

$$\varkappa \to - a k_1 \, \mathrm{tg}\left(a k_1 - \frac{m\pi}{2} - \frac{\pi}{4}\right) \tag{19}$$
$$\to |a k_1| \quad \text{for} \quad k_1 \to i\infty,$$

$$\begin{aligned}\lambda &\to \quad a k_2 \, \mathrm{ctg}[(b-a) k_2] \to - |a k_2| \\ \mu &\to \quad a k_2 \, \mathrm{tg}[(b-a) k_2] \to - |a k_2|\end{aligned}\Bigg\} \text{for } k_2 \to i\infty$$

With these expressions Eq. (11) yields:

$$\omega_p^2/\omega^2 \to 1 - (\lambda/\varkappa) \to 2 \quad \text{for} \quad k_2^2 \to -\infty \,. \tag{20}$$

The corresponding values of k_z are given by Eq. (3) for $\varepsilon_2 = 1$

$$k_z^2 = k_0^2 - k_2^2 \to \infty \,. \tag{21}$$

The last two equations show the existence of a resonance at $\omega^2 = \omega_p^2/2$ for arbitrary values of m, $b k_p$ and a/b, a feature which is well-known.

When $\varepsilon_2 \neq 1$ this resonance is given by

$$\omega_p^2/\omega^2 \to \varepsilon_2 + 1$$
$$k_z^2 = \varepsilon_2 k_0^2 - k_2^2 \to \infty \quad \text{for} \quad k_2^2 \to -\infty \,. \tag{22}$$

Close to resonance the large imaginary parts of k_1 and k_2 produce strong skin effect close to the plasma surface (surface waves).

The different character of the two types of modes above and below resonance is illustrated in Fig. 2 for $m = 1$. The two lowest waveguide-modes are labelled according to their behaviour at cut-off. Whereas for $\omega > \omega_p$ the electric field is stronger inside the plasma than on the outside the opposite is true for $\omega < \omega_p/\sqrt{2}$. Close to resonance the electric field is predominantly a short range field between narrow accumulations of surface charges. For $m = 0$ the fields have circular symmetry and the cut-off for the plasma guide mode is at $\omega = 0$. Otherwise the behaviour would be similar.

Group velocity

In many respects not only the phase velocity ω/k_z but also the group velocity $\mathrm{d}\omega/\mathrm{d}k_z$ will be of interest. In vacuum as well as in an empty waveguide the product of the two satisfies the relation

$$\frac{c^2}{v_{\mathrm{gr}} \cdot v_{\mathrm{ph}}} = c^2 \frac{k_z}{\omega} \frac{\mathrm{d}k_z}{\mathrm{d}\omega} = c^2 \frac{\mathrm{d}k_z^2}{\mathrm{d}\omega^2} = 1 \,. \tag{23}$$

The same relation even holds for a waveguide which is completely filled with the dielectric ε_1 of Eq. (1). We may therefore characterize the peculiarities in the behaviour of the group velocity by the quantity [10]

$$\delta = \frac{c^2}{v_{\mathrm{gr}} \cdot v_{\mathrm{ph}}} - 1 = c^2 \frac{\mathrm{d}k_z^2}{\mathrm{d}\omega^2} - 1 \tag{24}$$

which for a nondispersive and nonmagnetic medium has the value $\varepsilon - 1$. For a waveguide with dielectric loading according to Eq. (1) we have from Eqs. (24) and (3)

$$\delta = - c^2 \frac{\mathrm{d}k_2^2}{\mathrm{d}\omega^2} = - \frac{c^2}{b^2} \frac{\mathrm{d} t^2}{\mathrm{d}\omega^2} \tag{25}$$

i.e. δ is simply obtained from the derivative of the radial dispersion given by Eq. (11).
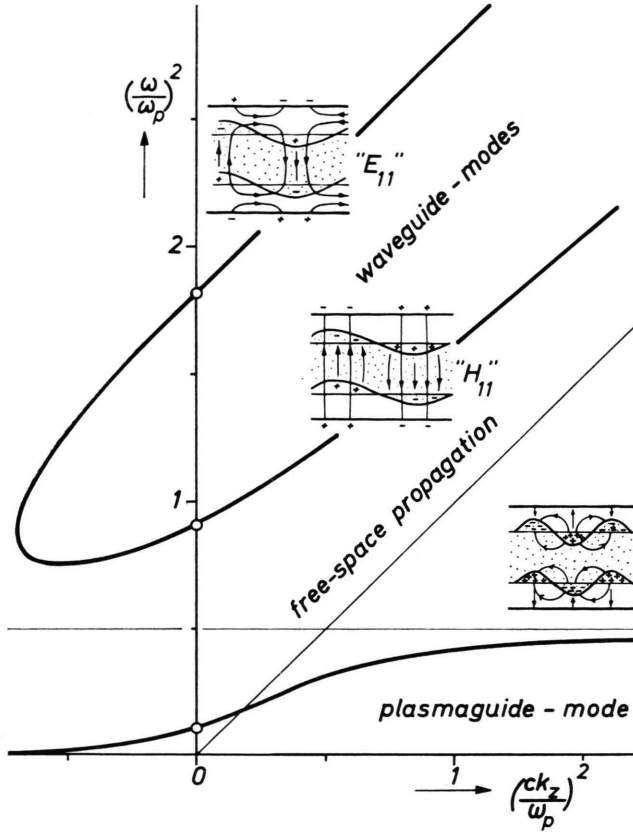
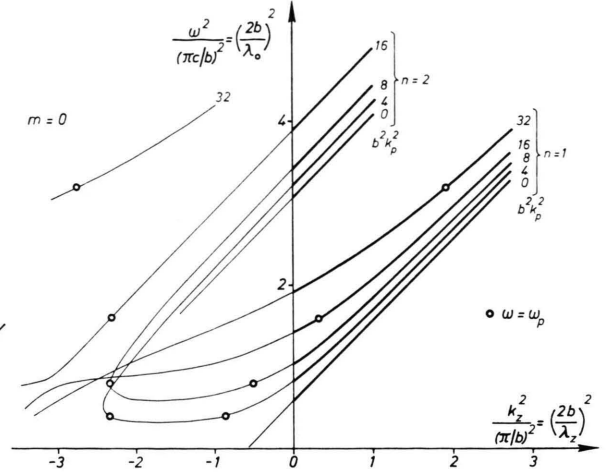Fig. 2. Waveguide and plasmaguide modes for $m = 1$ (schematic).

Fig. 3a. Axial dispersion of waveguide modes $m = 0$, $n = 1, 2$, $a/b = 1/2$ and different values of $b^2 k_p^2$.

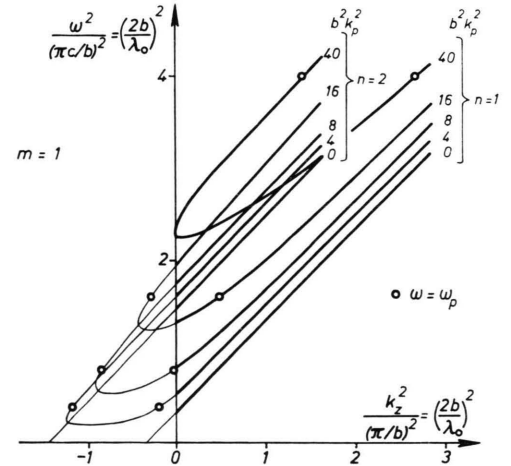Fig. 3b. Axial dispersion of waveguide modes $m = 1$, $n = 1, 2$, $a/b = 1/2$ and different values of $b^2 p^2$.

Effective dielectric constant

For practical considerations we can think of a homogeneous medium filling the waveguide completely and replacing the two dielectric zones in the sense that it produces the same k_z. This medium is then said to have the dielectric constant ε_{eff}:

$$k_z^2 = \varepsilon_{\text{eff}} k_0^2 - k_c^2 = k_0^2 \varepsilon_2 - k_2^2 = k_0^2 \varepsilon_1 - k_1^2 \quad (26)$$

where k_c is the cut-off wavenumber of the empty waveguide. Setting $\varepsilon_2 = 1$ we can define an "effective" average plasma frequency $\langle \omega_p^2 \rangle$ by

$$1 - \varepsilon_{\text{eff}} = \langle \omega_p^2 \rangle / \omega^2 = (k_2^2 - k_c^2)/k_z^2 . \quad (27)$$

Discussion of the Lowest Modes

The $m = 0$ modes

Setting $m = 0$ and multiplying both sides of Eq. (4) by the denominator of the right-hand side we obtain

$$(\varepsilon_1 t^2 \varkappa - \varepsilon_2 s^2 \lambda)(t^2 \varkappa - s^2 \mu) = 0 . \quad (28)$$

As we have done for $k_z = 0$, Eq. (15), we can distinguish between two cases:

Magnetic (TE) modes are obtained for

$$\varkappa/s^2 = \mu/t^2 . \quad (29)$$

Eq. (29) is identical with Eq. (17) for magnetic cut-off. The n-th root of Eqs. (29) and (10) can be written in the form

$$t_n^2 = t_n^2(b^2 k_p^2, a/b); \quad s_n^2 = t_n^2 - b^2 k_p^2 \quad (30)$$

and determines the radial dependence of the H_{0n} (TE$_{0n}$) modes. As the radial wavenumbers do not depend on ω for the assumed profile, the axial dispersion is of the same type as in an empty

waveguide:

$$k_z^2 = k_0^2 - t_n^2/b^2 \qquad (31)$$

i.e. in a diagram like that of Fig. 1 we would obtain a straight line parallel to the free-space propagation line and its cut-off frequency would be given by $\omega_c^2 = c^2 t_n^2/b^2$. The plasmaguide resonance at $\omega^2 = \omega_p^2/2$ is absent for these modes and from Eqs. (25) and (30) we conclude $\delta = 0$.

Electric (TM) modes are obtained for

$$\varepsilon_1 t^2 \varkappa - \varepsilon_2 s^2 \lambda = 0. \qquad (32)$$

Setting $\varepsilon_1 = 1 - \omega_p^2/\omega^2$, $\varepsilon_2 = 1$ we can solve for ω_p^2/ω^2 in the form

$$\omega_p^2/\omega^2 = 1 - \frac{s^2}{t^2} \cdot \frac{\lambda}{\varkappa}, \qquad s^2 = t^2 - b^2 k_p^2. \quad (33)$$

upon substituting Eqs. (5), (6), (9), and $\alpha = a/b$, one obtains the result,

$$\omega_p^2/\omega^2 = 1 - \frac{\alpha s J_0(\alpha s)}{J_1(\alpha s)} \frac{1}{t} \frac{J_1(\alpha t) N_0(t) - N_1(\alpha t) J_0(t)}{J_0(\alpha t) N_0(t) - N_0(\alpha t) J_0(t)}$$

$$(33\,\mathrm{a})$$

which would follow also from Eq. (11) for $m = 0$. Fig. 1a shows the corresponding plot for $a/b = 1/2$ and different values of $b k_p$.

In the $\omega^2 - k_z^2$-diagram it is convenient to plot the branches for $\omega^2/\omega_p^2 \gtrless 2$ separately and to distinguish between two kinds of modes (adopting the terminology of Ref. [2]):

$\omega^2/\omega_p^2 > 2$ or "waveguide modes"

These modes are illustrated in Fig. 3a from where it can be seen that they are relatively slight modifications of the modes of an empty waveguide. The plasma, roughly speaking, reduces the "electric width" of the waveguide and thereby increases its cut-off frequency. A natural frequency unit for these modes is $\pi c/b$, a natural unit for the wave-number being π/b. For large frequencies these modes have asymptotes which are parallel to the free-space propagation line $\omega^2 = c^2 k_z^2$. The $n = 1$ radial mode always approaches its asymptote from above and its slope is smaller than unity for $k_z^2 > 0$. From Eq. (24) we conclude $\delta > 0$. The $n = 2$ radial mode can approach its asymptote from below or from above (with $\delta \lessgtr 0$) depending on the values of $b k_p$. The transition occurs when the first poles of $\varkappa$ and λ coincide. For $a/b = 1/2$ this occurs around $b k_p = 4$.

$\omega^2/\omega_p^2 < 2$ or "plasmaguide modes"

These modes which we termed after Ref. [2] exhibit the resonance at $\omega^2 = \omega_p^2/2$. They owe their existence to the skin effect of the plasma and their natural frequency unit is ω_p. For $\omega^2 \ll \omega_p^2/2$ the plasma assumes the role of the metallic inner conductor of a coaxial line. In accordance with this picture the axisymmetric modes of Fig. 4a do not show low frequency cut-off. The limit $(b k_p)^2 = 0$ corresponds to the quasistatic approximation. This can be seen from Eqs. (2), (3) and (10)

$$b^2 k_z^2 \rightarrow - b^2 k_1^2 = - s^2,$$
$$b^2 k_0^2 \rightarrow 0: \qquad b^2 k_z^2 \rightarrow - b^2 k_2^2 = - t^2,$$
$$b^2 k_p^2/t^2 = (t^2 - s^2)/t^2 \rightarrow 0 \qquad (34)$$

(quasistatic approximation).

The $m = 1$ modes

All modes with $m \neq 0$ are generally of hybrid type and a clear discrimination between electric and magnetic modes is possible only at cut-off. Figs. 1 b, 3 b, 4 b are analogous to Figs. 1a, 3a, 4a for $m = 0$.
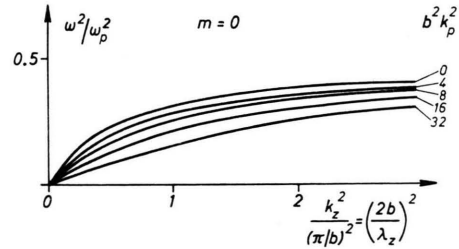

Fig. 4a. Axial dispersion of the plasmaguide mode $m = 0$, $a/b = 1/2$ and different values of $b^2 k_p^2$.
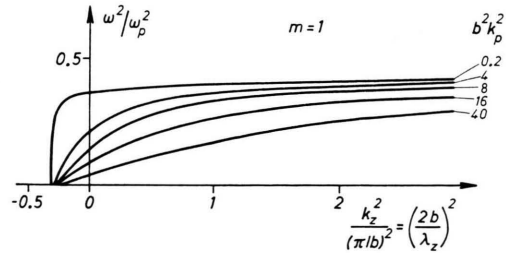

Fig. 4 b. Axial dispersion of the plasmaguide mode $m = 1$, $a/b = 1/2$ and different values of $b^2 k_p^2$.

For $m = 1$ the plasma guide mode shows cut-off as do the waveguide modes. The $m = 1$ modes can have regions of negative group velocity (backward waves)[1] however, the occurence of this is critically

dependent on the values of a/b and $b\,k_\mathrm{p}$. Numerical calculations for $a/b = 1/3$, which we do not present in detail, show backward wave regions for $b^2 k_p^2 \lesssim 1$ in the plasmaguide mode and for $b^2 k_p^2 \gtrsim 40$ for the $n = 1$ waveguide mode. From these calculations it seems that backward wave regions do not occur for a/b appreciably larger than $1/3$.

Low density approximation for the lowest radial waveguide modes

For $\omega_p^2/\omega^2 \ll 1$ and $(b\,k_\mathrm{p}/\pi)^2 \ll 1$ we can express the radial dispersion in the lowest powers of these quantities. This approximation simplifies the calculation of quantities of practical interest such as $k_z(\omega, \omega_\mathrm{p}, a, b)$.

$m = 0$: For the H_{01} (TE$_{01}$) mode the following relation is obtained by series expansion

$$t^2 = 14.7 + A_0 (b\,k_\mathrm{p})^2, \qquad (35)$$

$$1 - \varepsilon_\mathrm{eff} = \langle \omega_p^2 \rangle/\omega^2 = A_0 (\omega_\mathrm{p}/\omega)^2, \qquad (36)$$

and we have seen earlier that δ vanishes for all magnetic modes with $m = 0$. Table 1 gives approximate values of the constant [11] A_0.

Table 1.

a/b	1/3	1/2	2/3
A_0	0.1	0.33	0.7

For the E_{01} (TM$_{01}$) branch we obtain:

$$t^2 = 5.8 + A_0 (b\,k_\mathrm{p})^2 + A_1 (\omega_\mathrm{p}/\omega)^2 + A_2 (\omega_\mathrm{p}/\omega)^4. \quad (37)$$

From Eq. (35) we can derive approximate expressions for $1 - \varepsilon_\mathrm{eff}$ and with the help of Eqs. (27) and (25):

$$1 - \varepsilon_\mathrm{eff} = \langle \omega_p^2 \rangle/\omega^2$$
$$= (\omega_\mathrm{p}/\omega)^2 \{ A_0 + (b\,k_0)^{-2} [A_1 + A_2 (\omega_\mathrm{p}/\omega)^2] \}, \quad (38)$$

$$\delta = (b\,k_0)^{-2} \{ A_1 (\omega_\mathrm{p}/\omega)^2 + 2 A_2 (\omega_\mathrm{p}/\omega)^4 \}. \quad (39)$$

From the data of Fig. 2a and similar ones for other diameter ratios we found the following values for the coefficients A:

Table 2.

a/b	A_0	A_1	A_2
1/3	0.025	2.5	0
1/2	0.11	3.0	2.0
2/3	0.31	$3.4 + 0.2\,(b\,k_\mathrm{p})^2$	3.0

(For $a/b = 2/3$ an additional term is needed to make the approximation satisfactory.)

$m = 1$: For the H_{11} (TE$_{11}$)-like branch we find the following approximations

$$t^2 = 3.4 + (b\,k_\mathrm{p})^2 [B_0 + B_1 (\omega_\mathrm{p}/\omega)^2], \qquad (40)$$

$$1 - \varepsilon_\mathrm{eff} = \langle \omega_p^2 \rangle/\omega^2$$
$$= (\omega_\mathrm{p}/\omega)^2 \{ B_0 + B_1 (\omega_p^2/\omega^2) \}, \qquad (41)$$

$$\delta = (\omega_\mathrm{p}/\omega)^4 B_1, \qquad (42)$$

where the coefficients B are given in Table 3.

Table 3.

a/b	1/3	1/2	2/3	4/5	9/10
B_0	0.22	0.42	0.64	0.8	0.9
B_1	0.12	0.20	0.23	0.25	0.085

The following features seem to be noteworthy:

E_{01}: $1 - \varepsilon_\mathrm{eff}$ depends on $(\omega_\mathrm{p}/\omega)^2$ as well as on the vacuum wavelength-to-diameter ratio. For small densities δ is proportional to $(\omega_\mathrm{p}/\omega)^2$.

H_{11}-like: $1 - \varepsilon_\mathrm{eff}$ is — within the range of the approximation — not affected by the vacuum wavelength-to-diameter ratio. Moreover we find

$$1 - \varepsilon_\mathrm{eff} \to (a/b)(\omega_p^2/\omega^2) \quad \text{for} \quad (a/b) \to 1.$$

This means that the H_{11}-like mode in the case of a nearly filled waveguide averages with a weight given by the linear element of the diameter rather than the areal element of the cross section. For small densities δ is proportional to the square of the density.

Conclusions

The dispersion of a partly cold plasma filled circular waveguide has been studied by numerical solutions of the electromagnetic boundary value problem for the lowest radial modes with circular and dipole symmetry. The cases $\omega/\omega_\mathrm{p} \lesssim 1$ have been treated coherently. The calculations reveal the degree of accuracy of earlier calculations based on the quasistatic approximation. For low densities where $\omega_p^2/\omega^2 \ll 1$ as well as $\omega_p^2/\omega^2 \ll (\lambda_0/2b)^2$ is valid, the results of the calculations have been condensed into simple formulas which allow an easy estimate of phase and group velocity.

diagrams. Thanks are also due to Dr. H. DERFLER for discussions and Miss C. WALLNER for typing the manuscript.

[1] W. P. ALLIS, S. J. BUCHSBAUM and A. BERS, Waves in Anisotropic Plasmas, M.I.T. Press, Cambridge, Massachusetts 1963.

[2] A. W. TRIVELPIECE, Slow Wave Propagation in Plasma Waveguides, San Francisco Press Inc. 1967.

[3] A. W. TRIVELPIECE and R. W. GOULD, J. Appl. Phys. 30, 11 [1959]. (This article is also contained in Ref. [2].)

[4] B. O'BRIEN, R. W. GOULD and J. V. PARKER, Phys. Rev. Letters 14, 630 [1965].

[5] O. GEHRE, H. M. MAYER and M. TUTTER, Physics Letters 28 a, 35 [1968].

[6] O. GEHRE, H. M. MAYER and M. TUTTER, 9th International Conference on Ionization Phenomena in Gases, Bucharest 1969.

[7] We shall see that some of our results can easily be modified to include the case where ε_2 has a constant value $\neq 1$.

[8] A. SOMMERFELD, Vorlesungen über theoretische Physik Band III, Elektrodynamik, Dieterichsche Verlagsbuchhandlung, Wiesbaden 1948.

[9] J. D. JACKSON, Classical Electrodynamics, J. Wiley, New York 1962.

[10] In a subsequent publication we will show that δ is the quantity which determines the Fresnel effect i.e. the „drag,, exerted on the phase velocity when the refractive medium is given a translatory axial velocity in the laboratory system.

[11] The error for most coefficients in this and the following tables may be expected to be less than 10 percent.

Infrared Spectroscopy and Hydrogen Bonding: Complexing of γ-Butyrolactone with o-Cresol

G. NAGARAJAN

Department of Physics and Astronomy, Valdosta State College, Valdosta, Georgia, USA

Investigations to study the effect of different solvents on the frequency, intensity, and band width of the carbonyl band of γ-butyrolactone were carried out on the basis of the mixed solvent techniques with carbon tetrachloride, being the inert solvent. The solvent used for such investigations is o-cresol. The results establish the existence of the 1 : 1 and 1 : 2 complexes at fairly low concentrations for the γ-butyrolactone-o-cresol system. The formation constants for these complexes were determined and used to resolve the observed carbonyl bands into the spectra of individual complexes. The observed large frequency shift for the 1 : 2 complex favours a structure in which two molecules of o-cresol are directly bonded to the carbonyl group. The free energies of formation at 25 °C by using these formation constants show that the strength of the interaction increases in going from the 1 : 1 complex to the 1 :2 complex of the same γ-butyrolactone-o-cresol system. These results have been discussed in relation to the frequency shift, intensity changes, and half width changes.

Introduction

Experimental and theoretical investigations of solvent shifts for the various characteristic infrared absorption bands have been extensively carried out by many investigators but with results of conflicting nature on the solvent induced frequency shift as well as the variation in intensity and band width. A few investigators [1-4] interpreted the frequency shifts on the basis of the bulk dielectric properties of the solvents, while BELLAMY and WILLIAMS [5] did so on the basis of the specific (localized) solvent-solute interactions. Interpretations of the solvent induced frequency shifts were later given by CALDOW and THOMPSON [6] by taking into account both these bulk dielectric effects and specific interaction effects.

A comprehensive review of the current theories of solvent shifts and their experimental verifications has recently been published by WILLIAMS [7]. HORÁK and his associates [8, 9] explained the conditions for the applicability of various theories of solvent shifts of characteristic bands based on the reaction field model, proposed a new process known as the collision complexes, and provided evidence for the existence of weak complexes of phenol with nonpolar solvents. On the basis of the mixed solvent techniques initiated by BELLAMY and HALLAM [10], WHETSEL and KAGARISE [11, 12] calculated the individual spectra of 1:1 and 1:2 complexes by studying the different types of solute-solvent (weak as well as strong) interactions and concluded that the non-dipolar interactions such as the dispersion for-